6. APPENDICES

Appendix 1: LEED

Low energy electron diffraction is a powerful technique to analyse surface long-range ordered structures, since their reciprocal lattice can directly be acquired. It consists of a collimated electron beam impinging onto the sample with energies in the 20-300eV range. Electrons with these energies have corresponding de Broglie wavelengths comparable to the interatomic distances[21]. When low energy electrons reach the sample, they are elastically scattered only in the outermost (two or three) atomic layers following Bragg's law. Electrons scattered from deeper layers are mostly inelastically scattered before exiting the crystal. This is the main difference with diffraction of an electromagnetic wave such as X rays: electrons interact so much stronger with matter than photons that they can only elastically access the surface of the material, while X rays penetrate deeper into the solid and therefore can provide information about its bulk structure[22].

The LEED basic instrumental set up is shown in Figure 22. The gun emits electrons with a selected energy (monochromatic beam). When these electrons reach the sample, elastic and inelastic scattering is produced and electrons are backscattered in all directions. Since the electrons that carry structural information are elastically scattered, four filtering grids eliminate electrons with lower energies[23]. The remaining ones are accelerated to a fluorescent screen and generate patterns reflecting the dominant reciprocal lattices of the surface. UHV conditions are required in these experiments, to maintain a clean surface and to avoid unwanted scattering of electrons on their path.

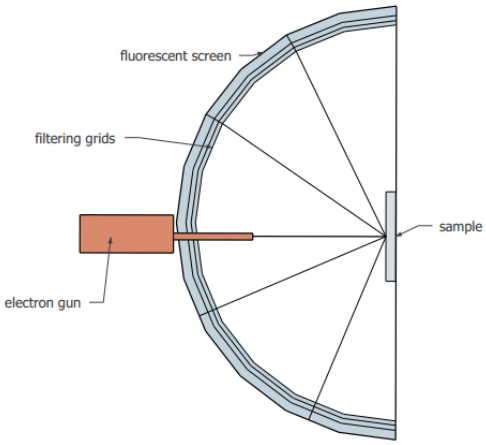

Figure 22. *Experimental set up of a LEED system.*

The Ewald construction is useful to visualize the conditions that must be satisfied by the reciprocal lattice and the electrons wave vector in order to observe diffraction (Fig. 23). It is constructed by drawing the incoming wave vector $\mathbf{k}_{00} = \frac{2\pi}{\lambda}\mathbf{n}$ in the direction of the incident beam (**n**) and ending in a reciprocal lattice point[22]. Then, a sphere (circle in 2 dimensions) is drawn with radius $|\mathbf{k}_{00}|$ and origin in the vector origin (see Fig. 23a). The elastically scattered waves will intersect with this sphere, matching the Laue diffraction condition and the conservation of energy. These are observed as light spots on the florescence screen and coincide with reciprocal lattice points. Imperfections in the lattice or dirt will contribute to the signal as featureless background.

In figure 23b, the reciprocal lattice of a surface is shown. Since the reciprocal lattice vector is inversely proportional to the real lattice vector (infinitesimal in length), the reciprocal lattice vector perpendicular to the surface has an infinite length. In other words, the reciprocal lattice of a surface is constructed by rods, not by spots[21]. Increasing the energy of electrons will increase $\mathbf{k}_{00}$, and thus the Ewald sphere radius, so that it can intersect with a higher number of rods.

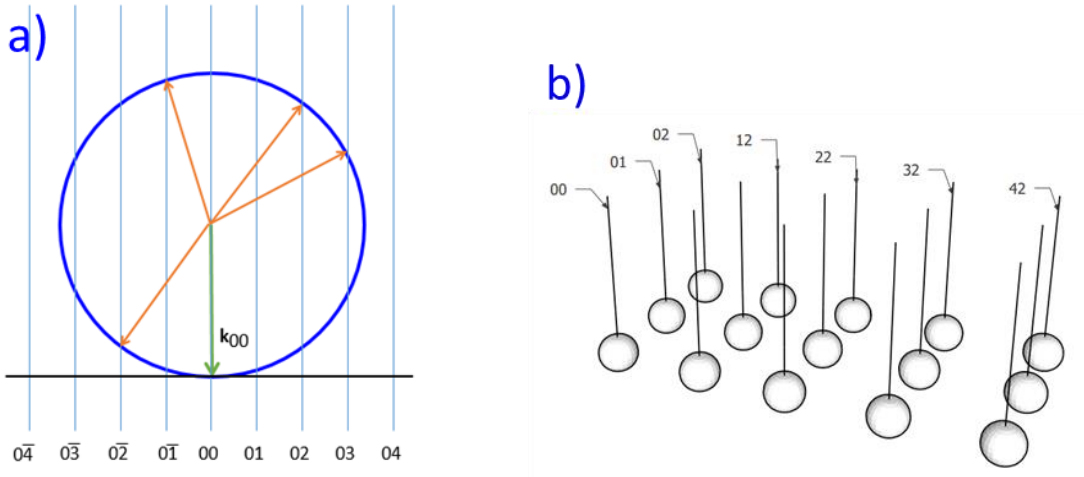

Figure 23. *a) Ewald construction for a surface projected onto a 2D plane. The incident wave vector is shown in green and some possible scattered wave vectors in orange. b) Reciprocal lattice of a surface, which is formed by rods.*

Appendix 2: Porous network LEED pattern

In this appendix we present the evolution of the LEED pattern of the molecular porous network as a function of energy. Figure 24 shows these patterns for different electron energy. The yellow hexagon highlights the molecular porous network unit cell while the green lines mark an incipient hexagons which corresponds to the pristine Cu(111) unit cell. The vectors of the Cu surface unit cell are 8 times larger than the molecular network ones. Then, we can deduce that the molecular porous network forms a (8x8) structure with respect to Cu(111).

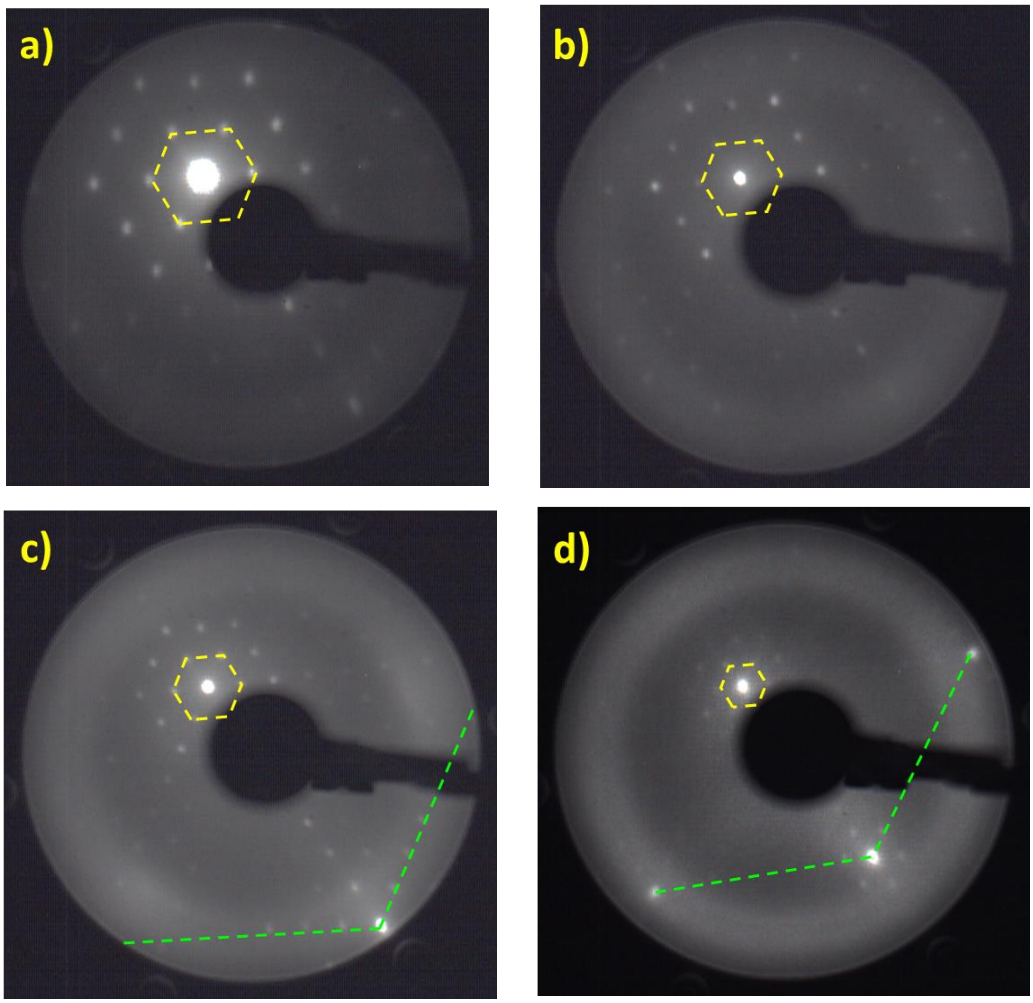

Figure 24. *LEED patterns of the porous network at different electron energies. Yellow dashed hexagons mark the 8x8 pattern and green lines mark the 1x1 one. a)E=25eV; b)E=40eV; c)E=60eV; d)E=100eV.*

Appendix 3: Profile heights of Co clusters

In this appendix we show the height profiles analysis performed to Co clusters as a function of the deposition order.

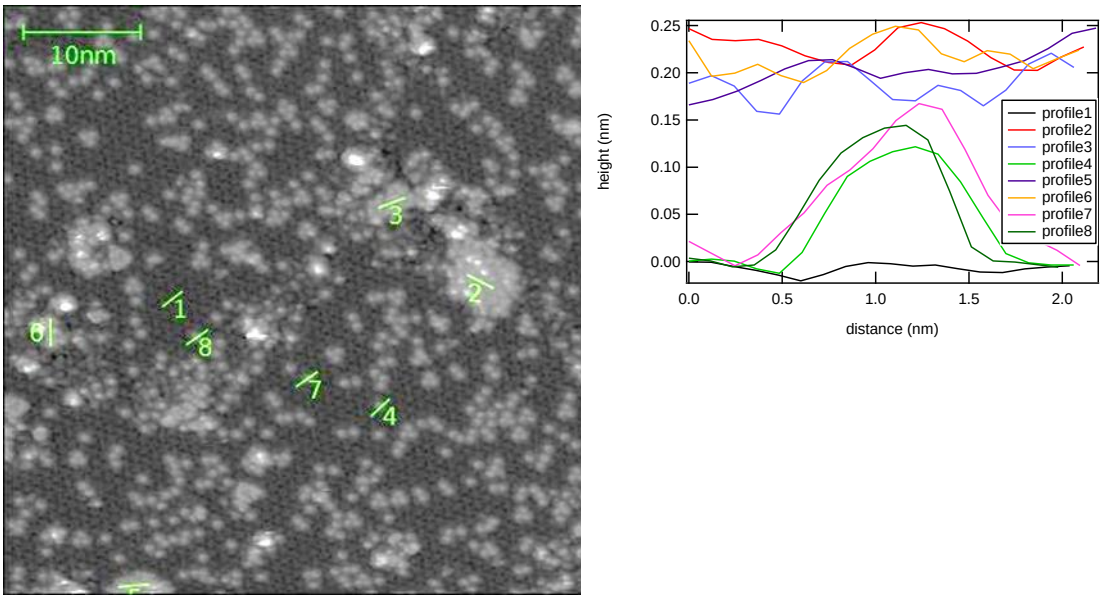

Figure 25. *Height analysis of different Co clusters in a* Co/DCA *system with* high coverage. *Scan details:* I_t*=50pA;* V_{bias}*=-0.2V; size=50x50nm*^{2}.

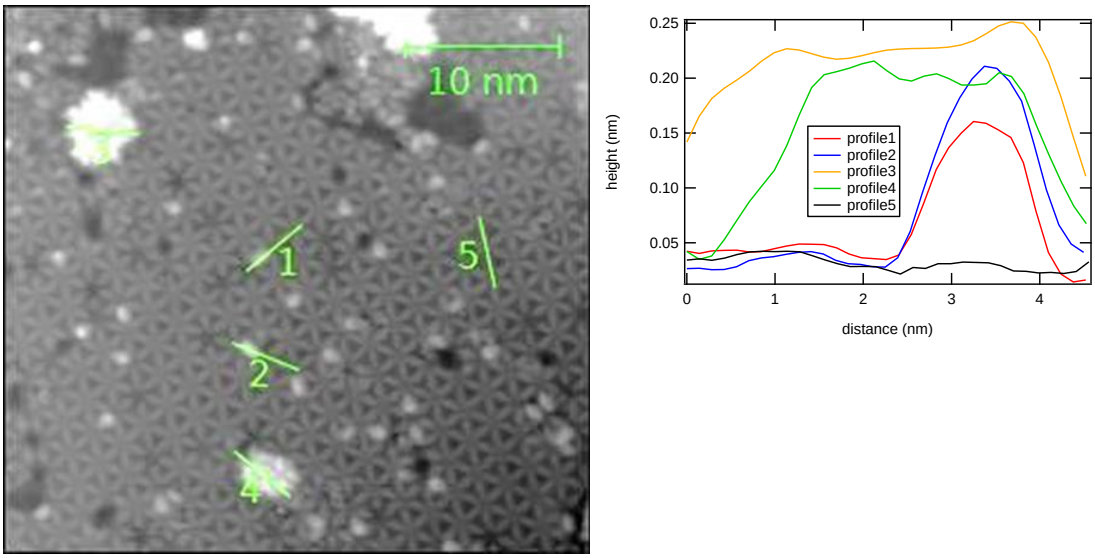

Figure 26. *Height analysis of different Co clusters in a* Co/DCA *system with* low coverage. *Scan details:* I_t*=50pA;* V_{bias}*=0.5V; size=40x40nm*^{2}.

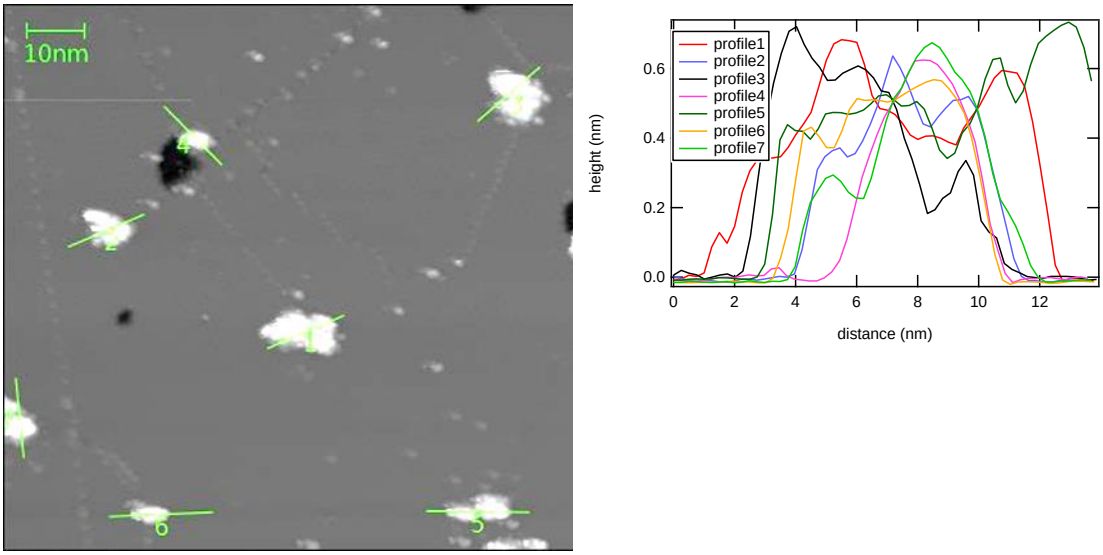

Figure 27. *Height analysis of different Co clusters in a* DCA/Co *system with* high coverage. *Scan details:* I_t*=120pA;* V_{bias}*=1V; size=100x100nm*^{2}.

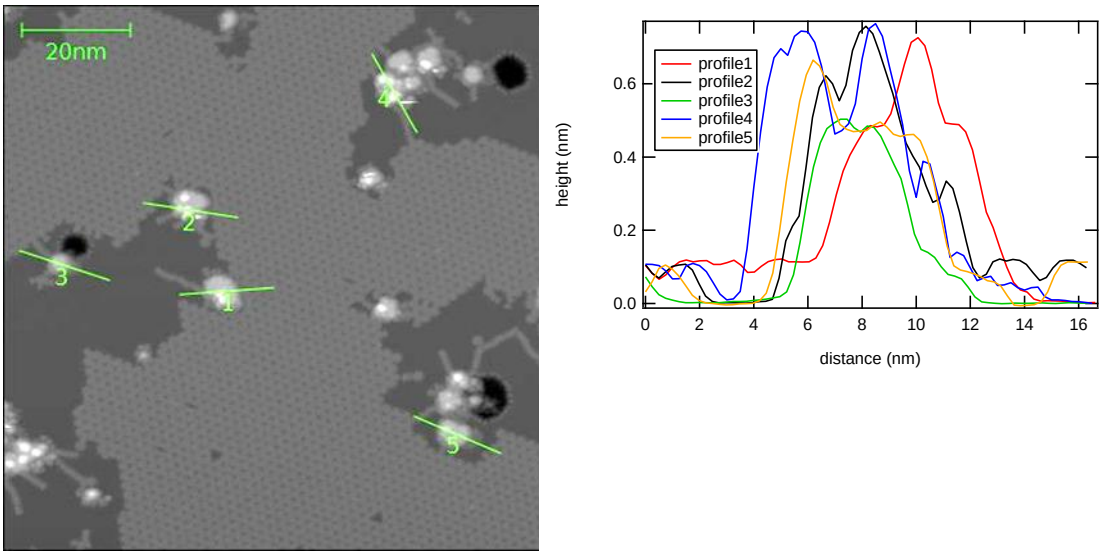

Figure 28. *Height analysis of different Co clusters in a* DCA/Co *system with* low coverage. *Scan details:* I_t*=120pA;* V_{bias}*=1V; size=100x100nm*^{2}.

In this analysis we can observe as in Co/DCA systems the clusters heights are around 0.2nm, which is the typical monoatomic height. However, DCA/Co systems show features higher than 0.6nm, which is clearly not monoatomic.

Appendix 4: Images Fe on pristine Cu(111)

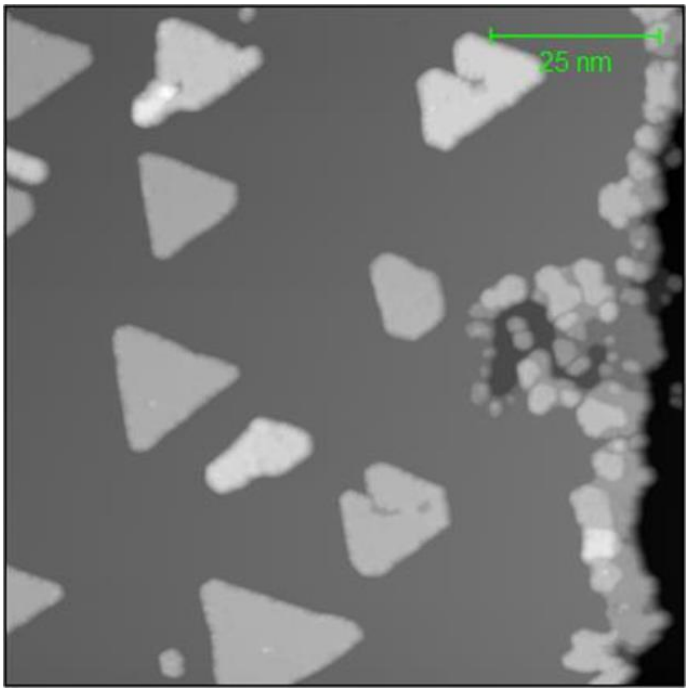

Figure 29. *Scan details: I_t=160pA; V_{bias}=1.5V; size=100x100nm^2.*

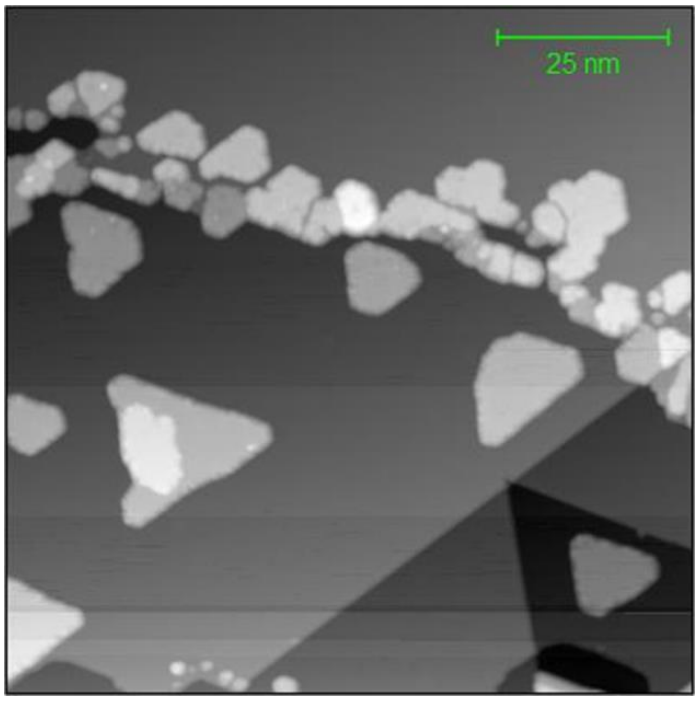

Figure 30. *Scan details: I_t=160pA; V_{bias}=1.5V; size=100x100nm^2.*